Proceedings of the ASME 2017 Fluids Engineering Division Summer Meeting
FEDSM2017
July 30-August 3, 2017, Waikoloa, Hawaii, USA

FEDSM2017-69041

USING DIRECT NUMERICAL SIMULATIONS FOR INVESTIGATING PHYSICS OF TURBULENCE IN POROUS MEDIA

Y. Jin
Center of Applied Space Technology and Microgravity (ZARM)
University of Bremen
Bremen, D-28359, Germany

A.V. Kuznetsov
Dept. of Mechanical & Aerospace Engineering
North Carolina State University
Raleigh, NC 27695-7910, USA

ABSTRACT

One of the most controversial topics in the field of convection in porous media is the issue of macroscopic turbulence. It remains unclear whether it can occur in porous media. It is difficult to carry out velocity measurements within porous media, as they are typically optically opaque. At the same time, it is now possible to conduct a definitive direct numerical simulation (DNS) study of this phenomenon. We examine the processes that take place in porous media at large Reynolds numbers, attempting to accurately describe them and analyze whether they can be labeled as true turbulence. In contrast to existing work on turbulence in porous media, which relies on certain turbulence models, DNS allows one to understand the phenomenon in all its complexity by directly resolving all the scales of motion.

Our results suggest that the size of the pores determines the maximum size of the turbulent eddies. If the size of turbulent eddies cannot exceed the size of the pores, then turbulent phenomena in porous media differ from turbulence in clear fluids. Indeed, this size limitation must have an impact on the energy cascade, for in clear fluids the turbulent kinetic energy is predominantly contained within large eddies.

INTRODUCTION

The topic of turbulence in porous media was reviewed in recent reference books on convection in porous media [1,2] and in many review chapters [3-6]. This topic is important in many applications, such as forestry (forest fires), agriculture engineering, chemical reactor design, catalytic converters, bio-filters, crude oil extraction, biomechanics of porous organs, and many others [7].

The first physically-based turbulence model was developed in [8]. This classical paper started the field of turbulence modeling in porous media. There are two distinct views on turbulence in porous media. The first view is expressed in [9] and [10]. According to this view, true macroscopic turbulence, at least in a dense porous medium, is impossible because of the limitation on the size of turbulent eddies imposed by the pore scale. This prevents the transfer of turbulent kinetic energy from larger to smaller turbulent eddies. Thus any turbulence in porous media is restricted to turbulence within the pores.

Although most published turbulence models attempt to obtain macroscopic characteristics of flow in porous media, some of them do this by simulating pore-scale turbulence. According to [10], the model developed by [11], due to the size of the periodic cell and the assumption of periodicity, in fact simulates turbulence within the pores. The same applies to [12].

The second class of models deals primarily with macroscopic turbulence in porous media. Representative models are those developed by [13,14] (there is a noteworthy discussion of the latter paper in [15]) as well as in [8,16]. Macroscopic turbulence models have also been used to simulate flow in a porous matrix represented by a periodic array of square cylinders [17,18].

Finally, many turbulence models attempt to simulate both pore-scale turbulence and large-scale turbulence. Representative models are those developed by M. de Lemos and colleagues, see [19-36].

Due to the opaque nature of the porous medium, there have been relatively few attempts to resolve turbulent flow in a porous medium experimentally. G.R. Thorpe's group [37,38] cleverly avoided this difficulty by studying a system where turbulence is generated by using a round water jet impinging on a porous foam. The authors reported Laser Doppler Velocimetry (LDV) measurements only in a fluid layer, but since the flow field in the fluid layer is affected by what is happening in the porous layer, the accuracy of predictions of the velocity field in the fluid layer can help indirectly judge the performance of the turbulence model in the porous layer.

Another possibility is to make a model porous medium out of transparent rods, use a viscous fluid with a refractive index similar to the refractive index of the rods, add some small

spherical particles to the flow, and perform a Particle Image Velocimetry. This idea was utilized to measure the velocity of a laminar flow in a porous medium [39-42]. The same idea was later used to study mean velocities and Reynolds stresses in a turbulent flow in a porous medium [43,44].

Refs. [45,46] investigated transition to turbulence in a flow of an electrolyte solution in a porous medium. By measuring current intensities from imbedded electrodes (an unsteady current was interpreted as the evidence of fluctuating velocity), the authors studied the evolution of velocity gradient fluctuations. With this technique, they were able to study the evolution of characteristic length scales of the flow for different Reynolds numbers. A similar idea, based on the utilization of an electrochemical technique, was used in [47].

Ref. [48] investigated the transition to turbulence in a pore-doublet model designed to mimic flow around one solid particle in a porous medium. A large pipe was split into two smaller pipes that formed a U-shaped geometry. Two pressure transducers recorded pressure drops over the smaller pipes.

Ref. [49] utilized Magnetic Resonance Imaging (MRI) to resolve the flow field in laminar and turbulent flows as well as passive scalar transport through porous fins. Unlike other methods, MRI allowed for resolving the flow field in a realistic, rather than idealized, geometry of the porous medium.

Ref. [50] used an Ultrasonic Velocity Profiler, a probe capable of measuring the average pore velocity, at a series of points along the pore. These authors also reported the two-point velocity statistics.

GENERIC POROUS MATRIX (GPM)

Recently we investigated whether macroscopic turbulence is possible in a porous medium by conducting a DNS study of a turbulent flow in a specially designed porous matrix [51]. The advantage of DNS is that it avoids any kind of turbulence modeling. The obtained results suggest that in a porous medium the size of turbulent structures is restricted by the pore scale. The pore scale prevalence hypothesis (PSPH) was proven by three independent techniques of analyzing turbulent length scales (two-point correlations, integral length scales, and pre-multiplied energy spectra).

The GPM-geometry that we used is shown in Fig. 1. It is built by a large number of rectangular bars of size $d \times d$ being s apart in both directions. Quite generally a porous matrix can be characterized by its representative elementary volume (REV) which is the smallest subvolume that shows the same behavior with respect to the flow through it as the flow that can be observed in the whole matrix. In a geometrically regular matrix the REV is of the order of the pore size when the flow is laminar. Such an REV is shown in Fig. 1 and labelled REV-L. However, when the flow is turbulent, some turbulent structures may be much larger than the REV-L, so that the appropriate REV, now labelled REV-T, is also much larger than REV-L. In Fig. 1 the REV-T occupies the whole area shown in Fig. 1.

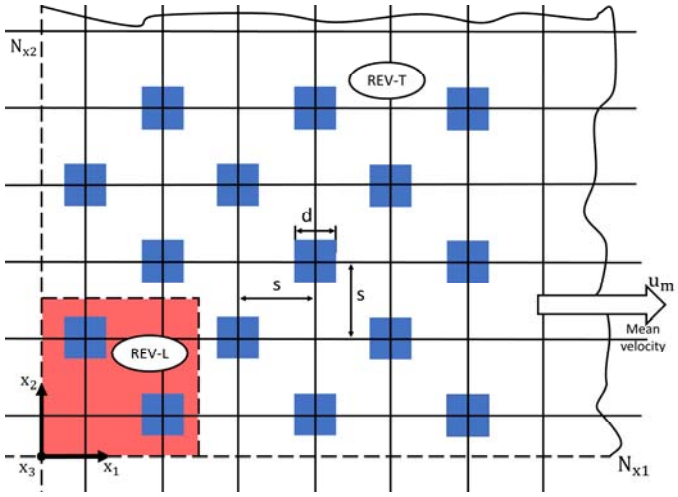

Figure 1. Schematic diagram of the GPM used in our DNS study. The GPM is shown here for five rows in the x_1-direction and four rows in the x_2-direction, together with the representative elementary volumes REV-L and REV-T.

DNS METHODS

Two different methods which complement and verify each other were applied to search for possible macroscopic turbulence in porous media. They are

- The finite volume method (FVM) which directly solves the Navier-Stokes equations.
- The Lattice-Boltzmann method (LBM) which determines the particle distribution. This method indirectly corresponds to solving the Navier-Stokes equations.

Both of the two DNS methods have second order accuracy in space and time. The Reynolds number was defined as

$$\mathrm{Re} = \frac{u_m d}{\nu}, \qquad (1)$$

where u_m and d are defined in Fig. 1 and ν is the kinematic viscosity of the fluid.

A measure of the overall accuracy of the DNS solution is Δ, which is defined as

$$\Delta = \frac{g_p - g_s}{g_p}, \qquad (2)$$

where g_p and g_s are the pressure gradients in the flow determined by evaluating the pressure in two opposing cross-sections (g_p) and by integrating the dissipation of the mechanical energy between them (g_s).

As explained in [51], for a perfect DNS solution the accuracy measure Δ would be zero since in such a case $g_p=g_s$. In real DNS g_s will always be smaller than g_p since not all scales are resolved and certain local dissipation effects are missing. For example, Δ values are 0.1%-1.5% for the DNS results for a flow in a channel with smooth walls while they are

7%-10% for more complicated turbulent flows such as a flow in a channel with rough walls [52,53].

TURBULENT LENGTH SCALES

Taking into account the requirements with respect to the REV-T as well as the available computational resources, we have performed low resolution DNS (domain size: $20d \times 20d \times 10d$; typical mesh resolution: $280 \times 280 \times 140$) and high resolution DNS studies (domain size: $12d \times 8d \times 4d$; typical mesh resolution: $1200 \times 800 \times 400$). The Reynolds numbers were from 500 to 1000. Periodic boundary conditions were imposed in all three directions. The FVM was used for low resolution DNS studies while both the FVM and the LBM were used for high resolution DNS studies. The numerical results show that the accuracy measure Δ was 20%-40% in the low resolution DNS studies and smaller than 10% in the high resolution DNS studies. However, domain sizes, mesh resolution and numerical methods do not have noticeable effect on the statistical results.

Turbulence is characterized by fluctuating flow quantities in a field that is strongly affected by eddy structures of various sizes, often called coherent structures. These coherent structures are the building blocks of turbulence and need to be identified when turbulence is analyzed in detail. We used three different methods to analyze the turbulent flow with respect to the scales that are involved.

Two-Point Correlations

This technique of turbulent length scale analysis uses two quantities of the same kind, which are a certain distance $\boldsymbol{r}$ apart. Fluctuation behavior of these quantities is observed. When b is such a quantity, its fluctuation b' is defined by the following equation

$$b = \langle b \rangle + b' , \tag{3}$$

where $\langle b \rangle$ is the time mean value of b. When two such fluctuating quantities b_1' and b_2' are considered, nonzero values of $\langle b_1' b_2' \rangle$ will occur when physical correlations of whatever kind exist. Analyzing $\langle b_1' b_2' \rangle$ can be used to detect flow structures in unsteadily fluctuating flow fields.

A two-point correlation between the quantities $b_i'(\boldsymbol{x})$ and $b_j'(\boldsymbol{x}+\boldsymbol{r})$ at a certain time t is called the two-point, one-time autocovariance. It is defined as

$$R_{ij}(\boldsymbol{r},\boldsymbol{x}) = \left\langle b_i'(\boldsymbol{x},t)\, b_j'(\boldsymbol{x}+\boldsymbol{r},t) \right\rangle . \tag{4}$$

For example, for velocity fluctuations $u_i'(\boldsymbol{x}_0,t)$ and $u_i'(\boldsymbol{x}_0+\boldsymbol{r},t)$, the two-point correlation is defined as

$$R_{ii}(\boldsymbol{r},\boldsymbol{x}_0) = \left\langle u_i'(\boldsymbol{x}_0,t)\, u_i'(\boldsymbol{x}_0+\boldsymbol{r},t) \right\rangle . \tag{5}$$

Fig. 2a shows such a correlation for the GPM displayed in Fig. 1 with the correlation point $\boldsymbol{x}_0$ in the middle of the computational domain. The correlation was calculated by time averaging of the FVM results for the Reynolds number of 500.

Non-zero correlations occur not solely from turbulent fluctuations but also due to simultaneous unsteady motions around each of the bars. They are called non-turbulent correlations and have to be distinguished from the true turbulent correlations due to the turbulent coherent structures. This can be done assuming that the non-turbulent correlations are the same for all values r_3, i.e. that $u_i'(\boldsymbol{x}_0,t)$ correlated with $u_i'(\boldsymbol{x}_0+\boldsymbol{r}+r_3\boldsymbol{e}_3,t)$ has the same non-turbulent correlation pattern. Adding $r_3\boldsymbol{e}_3$ to the correlation distance $\boldsymbol{r}$ means that now the correlation points are located in two parallel planes which are a distance r_3 apart. This special correlation is called a two-point lateral correlation, and is defined by

$$\tilde{R}_{ii}(r_3,\boldsymbol{r},\boldsymbol{x}_0) = \left\langle u_i'(\boldsymbol{x}_0,t)\, u_i'(\boldsymbol{x}_0+\boldsymbol{r}+r_3\boldsymbol{e}_3,t) \right\rangle . \tag{6}$$

When now $\tilde{R}_{ii}$, which is defined by Eq. (6), is subtracted from R_{ii}, which is defined by Eq. (5), the difference $R_{ii} - \tilde{R}_{ii}$ gives the true turbulent correlations providing that r_3 is so large that there are no correlations due to the large-scale turbulent structures in $\tilde{R}_{ii}$.

Thus, turbulent correlations can be identified by studying the following quantity

$$\hat{R}_{ii}(\boldsymbol{r},\boldsymbol{x}_0) = R_{ii}(\boldsymbol{r},\boldsymbol{x}_0) - \tilde{R}_{ii}(r_3 > r_{3c},\boldsymbol{r},\boldsymbol{x}_0) , \tag{7}$$

with r_{3c} being the critical value of r_3 up to which there is an influence of large-scale turbulent structures.

Fig. 2b shows R_{11}, $\tilde{R}_{11}$, and $\hat{R}_{11}$ for a part of the computational domain in Fig. 2a. Appreciable non-zero values of $\hat{R}_{11}$ only occur around $\boldsymbol{x}_0$ at a distance smaller than the pore scale s, indicating that Fig. 2b shows the REV-T for this case and that, at least here, the PSPH holds.

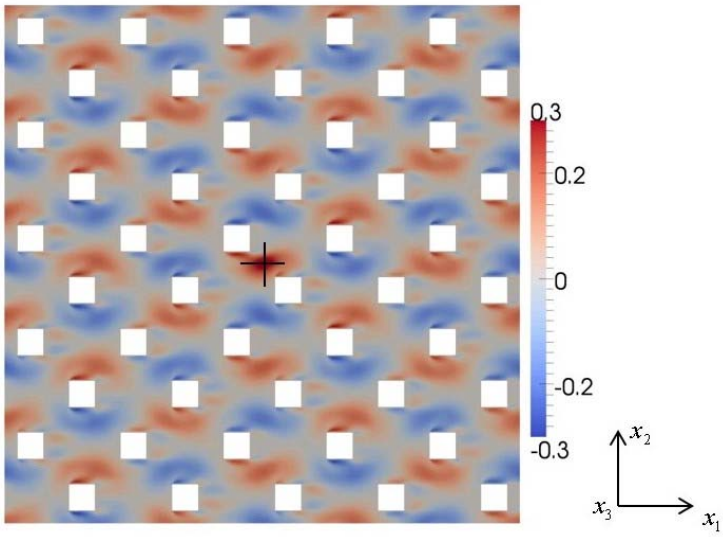

(a)

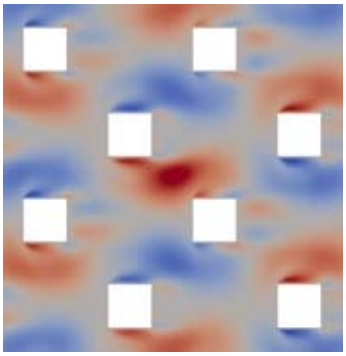

R_{11}/u_m^2

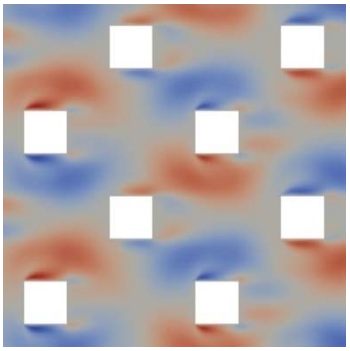

$\tilde{R}_{11}/u_m^2$

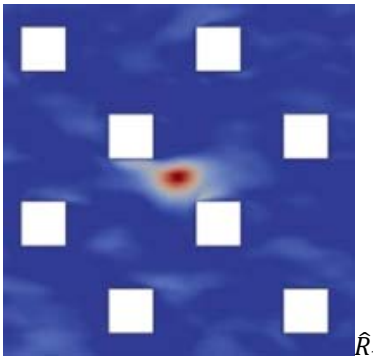

$\hat{R}_{11}/u_m^2$

$\hat{R}_{11}/u_m^2$

(b)Figure 2. Two-point correlations in the generic porous matrix; correlation point $\boldsymbol{x}_0$ marked by the cross in the middle; $s/d = 2, \mathrm{Re} = 500$, FVM-DNS. (a) Two-point correlation R_{11} in the whole computational domain, (b) Two-point correlations near the correlation point $\boldsymbol{x}_0$. R_{11}: Two-point correlation defined by Eq. (5); $\tilde{R}_{11}$: Two-point lateral correlation defined Eq. (6), $r_3 = 5d$; $\hat{R}_{11}$: Turbulent correlation defined by Eq. (7).

Integral Length Scales

Another way to quantify the size of large eddies is to determine their integral length scales. These length scales are defined as longitudinal, transverse and spanwise lengths L_{ii}, similar to the definitions in [54] for homogeneous and isotropic turbulent flows:

$$L_{ii} = \int_{-\infty}^{\infty} \hat{R}_{ii}\left(r_i \boldsymbol{e}_1, \boldsymbol{x}_0\right) \Big/ \hat{u}_i'^2\left(\boldsymbol{x}_0\right) dx_i \quad (i=1,2,3), \tag{8}$$

where $\hat{u}_i'\left(\boldsymbol{x}_0\right)$ is the root-mean-square turbulent velocity component, which is defined as

$$\hat{u}_i'\left(\boldsymbol{x}_0\right) = \hat{R}_{ii}\left(0, \boldsymbol{x}_0\right)^{1/2}. \tag{9}$$

These definitions were used despite the fact that the flow in porous media is not one with isotropic and homogeneous turbulence. However, since the analysis must provide only the order of magnitude of these length scales (whether they are of the pore or domain (REV-T) size), it was assumed that L_{ii} obtained from Eq. (8) were of the same order of magnitude as the corresponding length scales of the non-isotropic turbulence prevailing in porous media flows.

For the flow shown in Fig. 2 it was found that $L_{11} = 0.52s$, $L_{22} = 0.36s$, and $L_{33} = 0.21s$, again confirming the PSPH for this case.

Premultiplied Energy Spectra

For sufficiently large Reynolds numbers energy spectra have been derived by Kolmogorov (they are now called the Kolmogorov spectra) under the assumption of locally

homogeneous and isotropic turbulence being statistically in equilibrium. They are

$$\hat{E}_{ii}(\boldsymbol{x}_0, k_1) = \frac{1}{\pi}\int_{-\infty}^{\infty} \hat{R}_{ii}(x_1 \mathrm{e}_1, \boldsymbol{x}_0)\cos(k_1 x_1)\, dx_1 . \qquad (10)$$

Premultiplied energy spectra are the energy spectra multiplied by sk_1. These curves, which depict $sk_1\hat{E}_{ii}$ versus sk_1, plotted in semilogarithmic axes, have a distinct maximum with a corresponding wavelength Λ which indicates the wavelength and thus the size of the large scale energy-containing turbulent structures. For the flow shown in Fig. 2 the wavelengths in the three coordinate directions are $\Lambda = 2s$, $1.25s$ and $1.25s$, respectively. They are of the order of the REV-L size, see Fig. 1, which again confirms the PSPH for this case.

Visualization of Turbulent Structures

In Fig. 3 the so-called Q-method is used to visualize coherent structures in turbulent flows. Surfaces with constant values of Q/Q_m represent the vortex structure. The quantity Q is the second invariant of the instantaneous velocity gradient tensor. Q_m is the maximum value of Q. Iso-surfaces with larger Q/Q_m are closer to the vortex cores. Fig. 3 shows the transient flow structure in a part of the solution domain for the Reynolds of 1000. The high resolution LBM was used in this simulation.

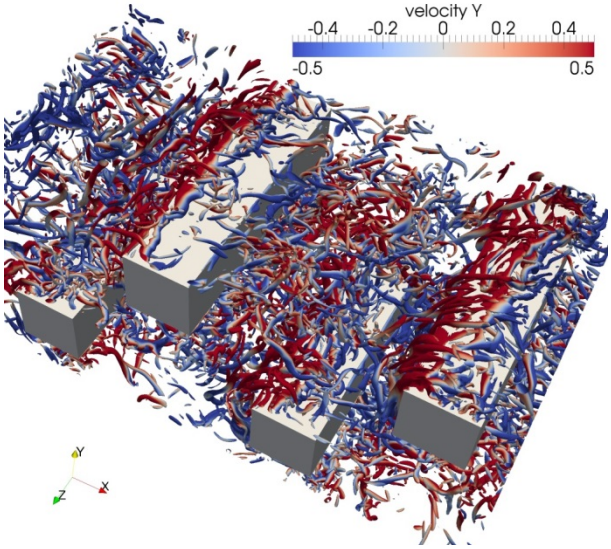

Figure 3. Snapshot of parts of the flow field in two REV-L elements (Re=1000, *s/d*=2), iso-surfaces $Q/Q_m = 0.011$, color coding shows the instantaneous value of the vertical velocity, u_2.

DIRECTIONS FOR FUTURE WORK

DNS results reported in this paper and in our previous work [51,55,56] suggest that any turbulence in porous media is restricted to turbulence within the pores. This finding presents the following questions:

- If this is true, does what is observed in porous media at large Reynolds numbers constitute true turbulence?
- What effects the additional production terms (due to solid obstacles) will have on turbulence?
- How the turbulent kinetic energy is transported to smaller eddies and then dissipated?
- It is well-known that most of turbulent kinetic energy is contained by large eddies, in the energy-containing range. If flow in a porous medium is turbulent, and there are no large eddies (due to size restrictions), how much turbulent kinetic energy is present in such a flow?
- If in a porous medium the turbulent kinetic energy is much smaller than in a clear fluid, how much influence turbulence has on the mean flow in a porous medium?
- What are the implications for heat transfer?
- Can turbulent flow in a porous medium exhibit some new fundamental features, not exhibited in a classical turbulent flow, such as the second critical Reynolds number in a bi-dispersed porous medium?
- How to model this phenomenon, in particular its effect on transport of thermal energy?

These topics should be addressed in future research.

ACKNOWLEDGMENTS

We gratefully acknowledge the support of this study by the DFG (Deutsche Forschungsgemeinschaft) and the HLRN (North-German Supercomputing Alliance). All the parallel computations in the present study were performed at the HLRN. AVK acknowledges with gratitude the support of the National Science Foundation (award CBET-1642262) and the Alexander von Humboldt Foundation through the Humboldt Research Award. We also appreciate valuable discussions with Prof. Heinz Herwig from TUHH.

REFERENCES

[1] de Lemos, M. J. S., 2012, *Turbulence in Porous Media: Modeling and Applications,* 2nd ed., Elsevier, Oxford, UK.

[2] Nield, D. A., and Bejan, A., 2013, *Convection in Porous Media,* 4th ed. ed., Springer, New York.

[3] Lage, J. L., de Lemos, M. J. S., and Nield, D. A., 2002, "Modeling turbulence in porous media," Ingham, D. B., and Pop, I. (Eds.), *Transport Phenomena in Porous Media II,* Elsevier, Oxford, UK, pp. 198-230.

[4] de Lemos, M. J. S., 2004, "Turbulent heat and mass transfer in porous media," Ingham, D. B., Bejan, A., Mamut, E., and Pop, I. (Eds.), *Technologies and Techniques in Porous Media,* Kluwer, Dordrecht, pp. 157-168.

[5] de Lemos, M. J. S., 2005, "The double-decomposition concept for turbulent transport in porous media," Ingham, D. B., and Pop, I. (Eds.), *In Transport Phenomena in Porous Media III,* Elsevier, Oxford, pp. 1-33.

[6] Vafai, K., Minkowycz, W. J., Bejan, A., 2006, "Synthesis of models for turbulent transport through porous media,"

Minkowycz, W. J., Sparrow, E. M., and Murthy, J. Y. (Eds.), *Handbook of Numerical Heat Transfer,* Wiley, New York, ch. 12.
[7] Lage, J. L., 1998, "The fundamental theory of flow through permeable media from Darcy to turbulence," Ingham, D. B., and Pop, I. (Eds.), *Transport Phenomena in Porous Media,* Pergamon, New York, pp. 1-30.
[8] Antohe, B., and Lage, J., 1997, "A General Two-Equation Macroscopic Turbulence Model for Incompressible Flow in Porous Media," International Journal of Heat and Mass Transfer, **40**(13), pp. 3013-3024.
[9] Nield, D. A., 1991, "The Limitations of the Brinkman-Forchheimer Equation in Modeling Flow in a Saturated Porous-Medium and at an Interface," International Journal of Heat and Fluid Flow, **12**(3), pp. 269-272.
[10] Nield, D., 2001, "Alternative Models of Turbulence in a Porous Medium, and Related Matters," Journal of Fluids Engineering-Transactions of the ASME, **123**(4), pp. 928-931.
[11] Nakayama, A., and Kuwahara, F., 1999, "A Macroscopic Turbulence Model for Flow in a Porous Medium," Journal of Fluids Engineering-Transactions of the ASME, **121**(2), pp. 427-433.
[12] Kuwahara, F., Kameyama, Y., Yamashita, S., 1998, "Numerical Modeling of Turbulent Flow in Porous Media using a Spatially Periodic Array," Journal of Porous Media, **1**(1), pp. 47-55.
[13] Lee, K., and Howell, J., 1991, "Theoretical and Experimental Heat and Mass-Transfer in Highly Porous-Media," International Journal of Heat and Mass Transfer, **34**(8), pp. 2123-2132.
[14] Prescott, P., and Incropera, F., 1995, "The Effect of Turbulence on Solidification of a Binary Metal Alloy with Electromagnetic Stirring," Journal of Heat Transfer-Transactions of the ASME, **117**(3), pp. 716-724.
[15] Lage, J., 1996, "The Effect of Turbulence on Solidification of a Binary Metal Alloy with Electromagnetic Stirring - Discussion," Journal of Heat Transfer-Transactions of the ASME, **118**(4), pp. 996-996.
[16] Getachew, D., Minkowycz, W., and Lage, J., 2000, "A Modified Form of the Kappa-Epsilon Model for Turbulent Flows of an Incompressible Fluid in Porous Media," International Journal of Heat and Mass Transfer, **43**(16), pp. 2909-2915.
[17] Kazerooni, R. B., and Hannani, S. K., 2009, "Simulation of Turbulent Flow through Porous Media Employing a v2f Model," Scientia Iranica Transaction B-Mechanical Engineering, **16**(2), pp. 159-167.
[18] Kundu, P., Kumar, V., and Mishra, I. M., 2014, "Numerical Modeling of Turbulent Flow through Isotropic Porous Media," International Journal of Heat and Mass Transfer, **75**, pp. 40-57.
[19] de Lemos, M., and Braga, E., 2003, "Modeling of Turbulent Natural Convection in Porous Media," International Communications in Heat and Mass Transfer, **30**(5), pp. 615-624.
[20] de Lemos, M., and Mesquita, M., 2003, "Turbulent Mass Transport in Saturated Rigid Porous Media," International Communications in Heat and Mass Transfer, **30**(1), pp. 105-113.
[21] Pedras, M., and de Lemos, M., 2000, "On the Definition of Turbulent Kinetic Energy for Flow in Porous Media," International Communications in Heat and Mass Transfer, **27**(2), pp. 211-220.
[22] de Lemos, M., and Pedras, M., 2001, "Recent Mathematical Models for Turbulent Flow in Saturated Rigid Porous Media," Journal of Fluids Engineering-Transactions of the ASME, **123**(4), pp. 935-940.
[23] Rocamora, F., and de Lemos, M., 2000, "Analysis of Convective Heat Transfer for Turbulent Flow in Saturated Porous Media," International Communications in Heat and Mass Transfer, **27**(6), pp. 825-834.
[24] de Lemos, M., and Tofaneli, L., 2004, "Modeling of Double-Diffusive Turbulent Natural Convection in Porous Media," International Journal of Heat and Mass Transfer, **47**(19-20), pp. 4233-4241.
[25] Pedras, M., and de Lemos, M., 2001, "Macroscopic Turbulence Modeling for Incompressible Flow through Undeformable Porous Media," International Journal of Heat and Mass Transfer, **44**(6), pp. 1081-1093.
[26] Pedras, M., and de Lemos, M., 2001, "On the Mathematical Description and Simulation of Turbulent Flow in a Porous Medium Formed by an Array of Elliptic Rods," Journal of Fluids Engineering-Transactions of the ASME, **123**(4), pp. 941-947.
[27] Pedras, M., and de Lemos, M., 2001, "Simulation of Turbulent Flow in Porous Media using a Spatially Periodic Array and a Low Re Two-Equation Closure," Numerical Heat Transfer Part A-Applications, **39**(1), pp. 35-59.
[28] Pedras, M., and de Lemos, M., 2003, "Computation of Turbulent Flow in Porous Media using a Low-Reynolds k-Epsilon Model and an Infinite Array of Transversally Displaced Elliptic Rods," Numerical Heat Transfer Part A-Applications, **43**(6), pp. 585-602.
[29] Silva, R., and de Lemos, M., 2003, "Turbulent Flow in a Channel Occupied by a Porous Layer Considering the Stress Jump at the Interface," International Journal of Heat and Mass Transfer, **46**(26), pp. 5113-5121.
[30] Braga, E. J., and de Lemos, M. J. S., 2006, "Simulation of Turbulent Natural Convection in a Porous Cylindrical Annulus using a Macroscopic Two-Equation Model," International Journal of Heat and Mass Transfer, **49**(23-24), pp. 4340-4351.
[31] Braga, E. J., and de Lemos, M. J. S., 2008, "Computation of Turbulent Free Convection in Left and Right Tilted Porous Enclosures using a Macroscopic k-Epsilon Model," International Journal of Heat and Mass Transfer, **51**(21-22), pp. 5279-5287.
[32] Graminho, D. R., and de Lemos, M. J. S., 2009, "Simulation of Turbulent Impinging Jet into a Cylindrical Chamber with and without a Porous Layer at the Bottom,"

International Journal of Heat and Mass Transfer, **52**(3-4), pp. 680-693.
[33] Saito, M. B., and de Lemos, M. J. S., 2010, "A Macroscopic Two-Energy Equation Model for Turbulent Flow and Heat Transfer in Highly Porous Media," International Journal of Heat and Mass Transfer, **53**(11-12), pp. 2424-2433.
[34] de Lemos, M. J. S., 2011, "Simulation of Turbulent Combustion in Porous Materials with One- and Two-Energy Equation Models," Heat Transfer in Multi-Phase Materials, **2**, pp. 443-460.
[35] Pivem, A. C., and de Lemos, M. J. S., 2013, "Turbulence Modeling in a Parallel Flow Moving Porous Bed," International Communications in Heat and Mass Transfer, **48**, pp. 1-7.
[36] de Lemos, M. J. S., and Pivem, A. C., 2014, "Turbulent Heat Transfer in a Counterflow Moving Porous Bed using a Two-Energy Equation Model," International Journal of Heat and Mass Transfer, **72**, pp. 98-113.
[37] Prakash, M., Turan, O. F., Li, Y. G., 2001, "Impinging Round Jet Studies in a Cylindrical Enclosure with and without a Porous Layer: Part I - Flow Visualisations and Simulations," Chemical Engineering Science, **56**(12), pp. 3855-3878.
[38] Prakash, M., Turan, O. F., Li, Y. G., 2001, "Impinging Round Jet Studies in a Cylindrical Enclosure with and without a Porous Layer: Part II - LDV Measurements and Simulations," Chemical Engineering Science, **56**(12), pp. 3879-3892.
[39] Tachie, M., James, D., and Currie, I., 2003, "Velocity Measurements of a Shear Flow Penetrating a Porous Medium," Journal of Fluid Mechanics, **493**, pp. 319-343.
[40] Tachie, M., James, D., and Currie, I., 2004, "Slow Flow through a Brush," Physics of Fluids, **16**(2), pp. 445-451.
[41] Agelinchaab, M., Tachie, M., and Ruth, D., 2006, "Velocity Measurement of Flow through a Model Three-Dimensional Porous Medium," Physics of Fluids, **18**(1), pp. 017105.
[42] Arthur, J. K., Ruth, D. W., and Tachie, M. F., 2009, "PIV Measurements of Flow through a Model Porous Medium with Varying Boundary Conditions," Journal of Fluid Mechanics, **629**, pp. 343-374.
[43] Bejatovic, S., Agelinchaab, M., and Tachie, M. F., 2009, "Experimental Study of Turbulent Flow through Two-Dimensional Porous Media," *Proceedings of ASME 2009 Fluids Engineering Division Summer Meeting,*. FEDSM2009-78292, pp. 1419-1428.
[44] Bejatovic, S., Tachie, M. F., Agelinchaab, M., 2010, "PIV Study of Turbulent Flow in Porous Media," Turbulence and Interactions, **110**, pp. 71-78.
[45] Seguin, D., Montillet, A., and Comiti, J., 1998, "Experimental Characterisation of Flow Regimes in various Porous Media - I: Limit of Laminar Flow Regime," Chemical Engineering Science, **53**(21), pp. 3751-3761.
[46] Seguin, D., Montillet, A., Comiti, J., 1998, "Experimental Characterization of Flow Regimes in various Porous Media - II: Transition to Turbulent Regime," Chemical Engineering Science, **53**(22), pp. 3897-3909.
[47] Yang, J., Bu, S., Dong, Q., 2015, "Experimental Study of Flow Transitions in Random Packed Beds with Low Tube to Particle Diameter Ratios," Experimental Thermal and Fluid Science, **66**, pp. 117-126.
[48] Khayamyan, S., Lundstrom, T. S., and Gustavsson, L. H., 2014, "Experimental Investigation of Transitional Flow in Porous Media with Usage of a Pore Doublet Model," Transport in Porous Media, **101**(2), pp. 333-348.
[49] Coletti, F., Muramatsu, K., Schiavazzi, D., 2014, "Fluid Flow and Scalar Transport through Porous Fins," Physics of Fluids, **26**(5), pp. 055104.
[50] Horton, N. A., and Pokrajac, D., 2009, "Onset of Turbulence in a Regular Porous Medium: An Experimental Study," Physics of Fluids, **21**(4), pp. 045104.
[51] Jin, Y., Uth, M. F., Kuznetsov, A. V., 2015, "Numerical Investigation of the Possibility of Macroscopic Turbulence in Porous Media: A Direct Numerical Simulation Study," Journal of Fluid Mechanics, **766**, pp. 76-103.
[52] Jin, Y., and Herwig, H., 2014, "Turbulent Flow and Heat Transfer in Channels with Shark Skin Surfaces: Entropy Generation and its Physical Significance," International Journal of Heat and Mass Transfer, **70**, pp. 10-22.
[53] Jin, Y., Uth, M. F., and Herwig, H., 2015, "Structure of a Turbulent Flow through Plane Channels with Smooth and Rough Walls: An Analysis Based on High Resolution DNS Results," Computers & Fluids, **107**, pp. 77-88.
[54] Pope, S. B., 2000, *Turbulent Flows,* Cambridge University Press, Cambridge, UK.
[55] Uth, M. F., Jin, Y., Kuznetsov, A. V., 2016, "A Direct Numerical Simulation Study on the Possibility of Macroscopic Turbulence in Porous Media: Effects of Different Solid Matrix Geometries, Solid Boundaries, and Two Porosity Scales," Physics of Fluids, **28**(6), pp. 065101.
[56] Jin, Y., and Kuznetsov, A. V., 2017, "Turbulence Modeling for Flows in Wall Bounded Porous Media: An Analysis Based on Direct Numerical Simulations," Physics of Fluids, doi: 10.1063/1.4979062, in press.